Electronic Supplementary Material (ESI) for Physical Chemistry Chemical Physics.
This journal is © the Owner Societies 2015

Supporting information for

"Amylin-Aβ oligomers at atomic resolution using molecular dynamics simulations: a link between Type 2 diabetes and Alzheimer's disease"

Michal Baram,[1,2] Yoav Atsmon-Raz, [1,2] Buyong Ma,[3] Ruth Nussinov[,3,4] and Yifat Miller*[,1,2]*

[1] Department of Chemistry and [2] Ilse Katz Institute for Nanoscale Science and Technology, Ben-Gurion University of the Negev, Beér-Sheva 84105, Israel.

[3] Basic Science Program, Leidos Biomedical Research, Inc. Cancer and Inflammation Program, National Cancer Institute, Frederick, MD 21702, USA

[4] Sackler Inst. of Molecular Medicine Department of Human Genetics and Molecular Medicine Sackler School of Medicine, Tel Aviv University, Tel Aviv 69978, Israel

*Corresponding authors:
Yifat Miller, Department of Chemistry and Ilse Katz Institute for Nanoscale Science and Technology, Ben-Gurion University of the Negev, Beér-Sheva 84105, Israel.
Tel: 972-86428705 Email: ymiller@bgu.ac.il
Ruth Nussinov, Basic Science Program, Leidos Biomedical Research, Inc. Cancer and Inflammation Program, National Cancer Institute, Frederick, MD 21702, USA
Sackler Inst. of Molecular Medicine Department of Human Genetics and Molecular Medicine Sackler School of Medicine, Tel Aviv University, Tel Aviv 69978, Israel
Tel: +1 301 846 5579 Email: NussinoR@helix.nih.gov

Table S1: Conformational energies of the simulated $A\beta_{1-42}$-$Amylin_{1-37}$ oligomers, computed from GMBV method.

Model	Energy (kcal/mol)	Standard deviation (kcal/mol)	Population (%)
B1	-11809	204	5.2
B2	-11745	199	4.8
B3	-11323	200	2.2
B4	-11546	203	3.6
B5	-11801	193	5.1
B6	-11057	204	0.9
B7	-11196	195	1.5
B8	-11620	206	4.1
C1	-11769	204	5.0
C2	-11620	189	4.1
C3	-11430	201	2.8
C4	-11440	205	2.9
C5	-11231	187	1.6
C6	-11031	214	0.8
C7	-11609	201	4.0
C8	-11496	213	3.3
D1	-11594	201	3.9
D2	-11681	194	4.5
D3	-11285	202	1.9
D4	-11407	203	2.7
D5	-10991	203	0.7
D6	-11059	195	0.9
D7	-11723	206	4.7
D8	-11489	208	3.2
E1	-11575	198	3.8
E2	-11699	201	4.6
E3	-11417	199	2.7
E4	-11394	195	2.6
E5	-11598	228	3.9
E6	-11023	205	0.8
E7	-11539	212	3.6
E8	-11521	219	3.4

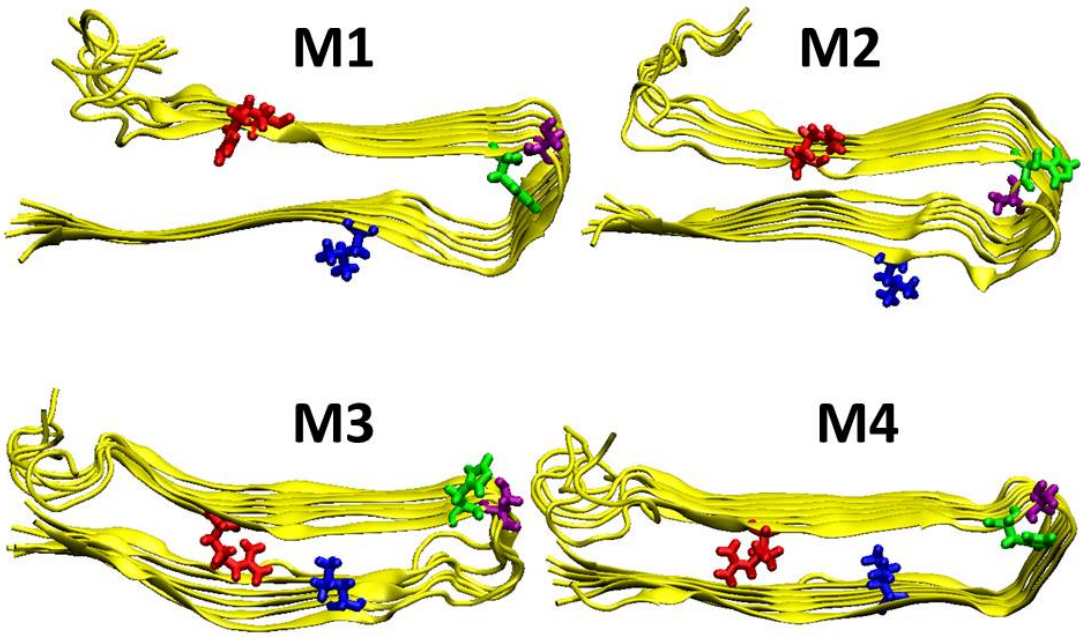

Figure S1: Constructed models M1-M4 of fibril-like of Amylin hexamer obtained from Miller's structures (Ref. 1) [based on Tycko's ssNMR (Ref. 2) and Eisenberg's crystal structures (Ref. 3)].

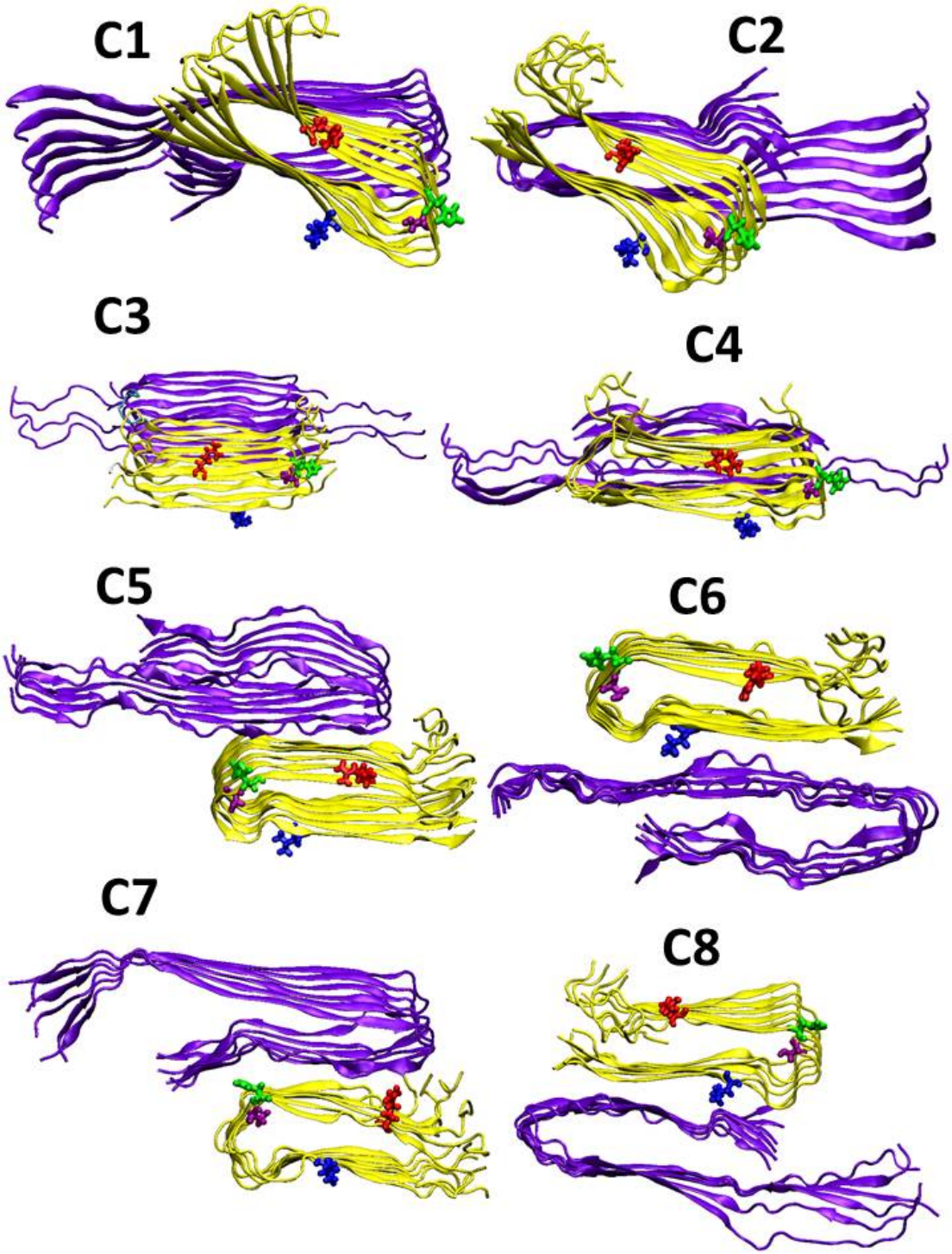

Figure S2: Constructed initial $A\beta_{1\text{-}42}$-$Amylin_{1\text{-}37}$ dodecamers. Aβ hexamer is based on Tycko structure (Ref. 4) and the Amylin hexamer M2 obtained from Miller's structures (Ref. 1) [based on Tycko's ssNMR (Ref. 2) and Eisenberg's crystal structures (Ref. 3)]. Models C1-C4 are single later conformations and C5-C8 are double layer conformations.

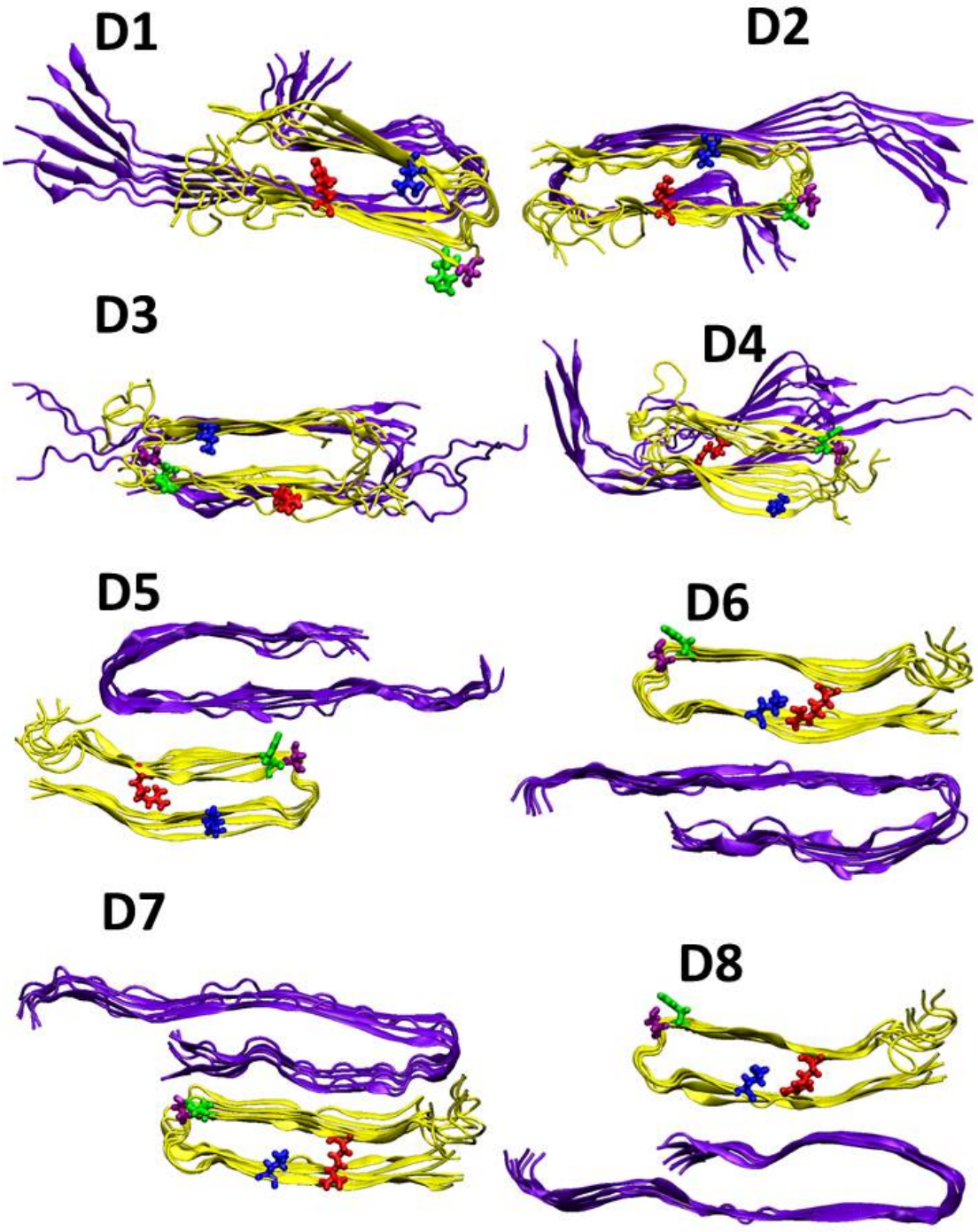

Figure S3: Constructed initial $A\beta_{1\text{-}42}$-$Amylin_{1\text{-}37}$ dodecamers. Aβ hexamer is based on Tycko structure (Ref. 4) and the Amylin hexamer M3 obtained from Miller's structures (Ref. 1) [based on Tycko's ssNMR (Ref. 2) and Eisenberg's crystal structures (Ref. 3)]. Models D1-D4 are single later conformations and D5-D8 are double layer conformations.

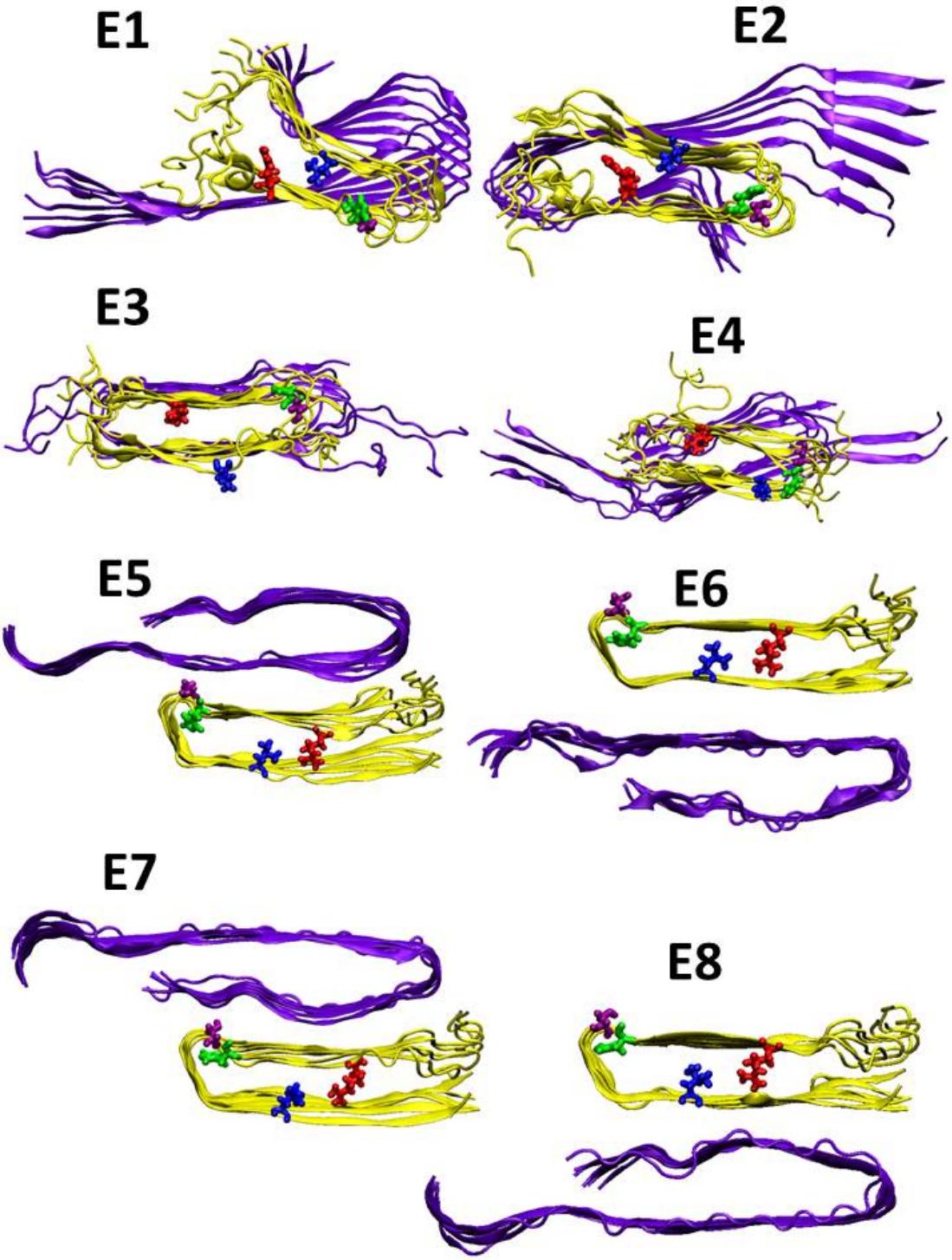

Figure S4: Constructed initial $A\beta_{1\text{-}42}$-$Amylin_{1\text{-}37}$ dodecamers. Aβ hexamer is based on Tycko structure (Ref. 4) and the Amylin hexamer M4 obtained from Miller's structures (Ref. 1) [based on Tycko's ssNMR (Ref. 2) and Eisenberg's crystal structures (Ref. 3)]. Models E1-E4 are single later conformations and E5-E8 are double layer conformations.

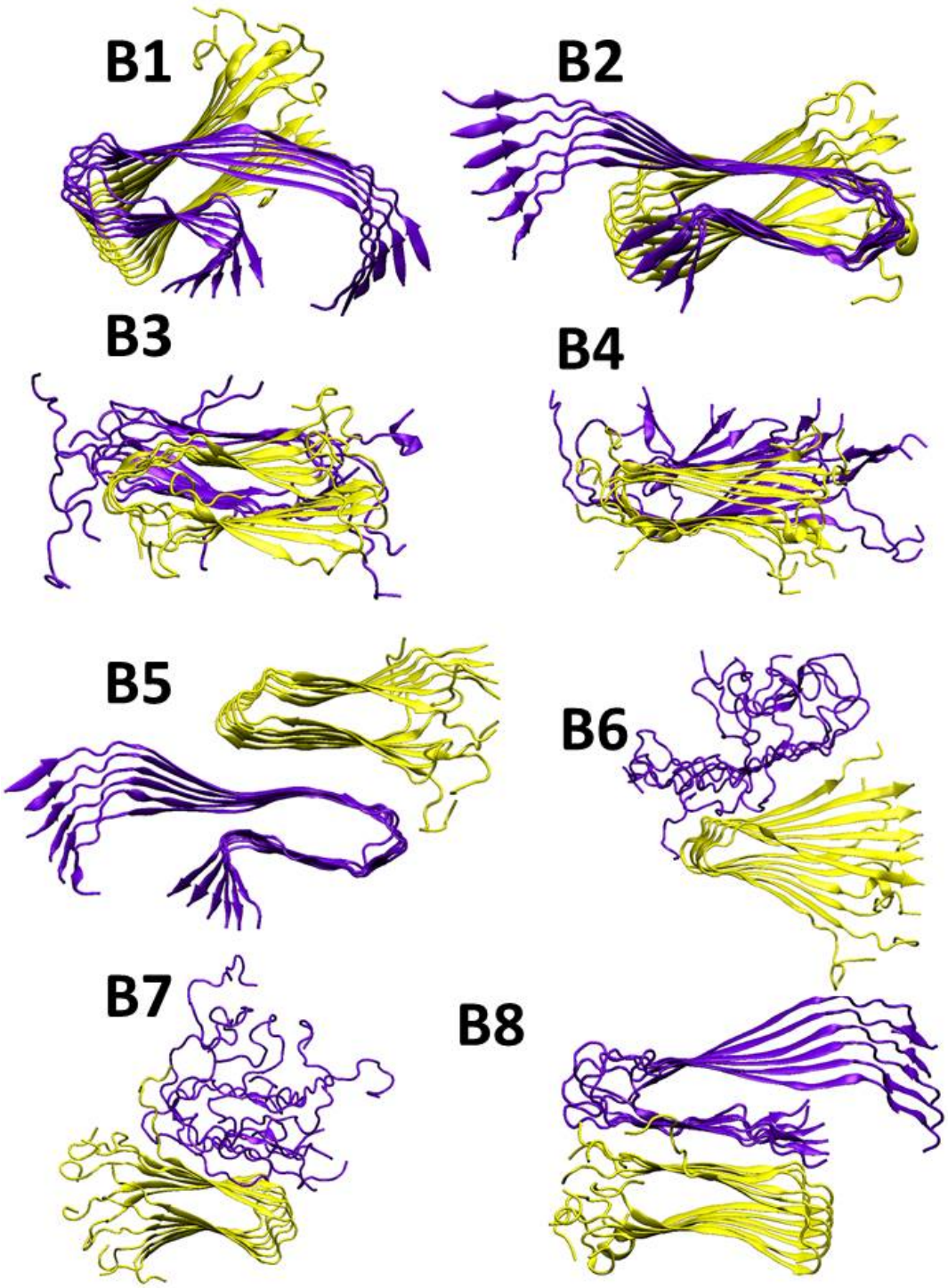

Figure S5: Simulated $A\beta_{1\text{-}42}$-$Amylin_{1\text{-}37}$ dodecamers.

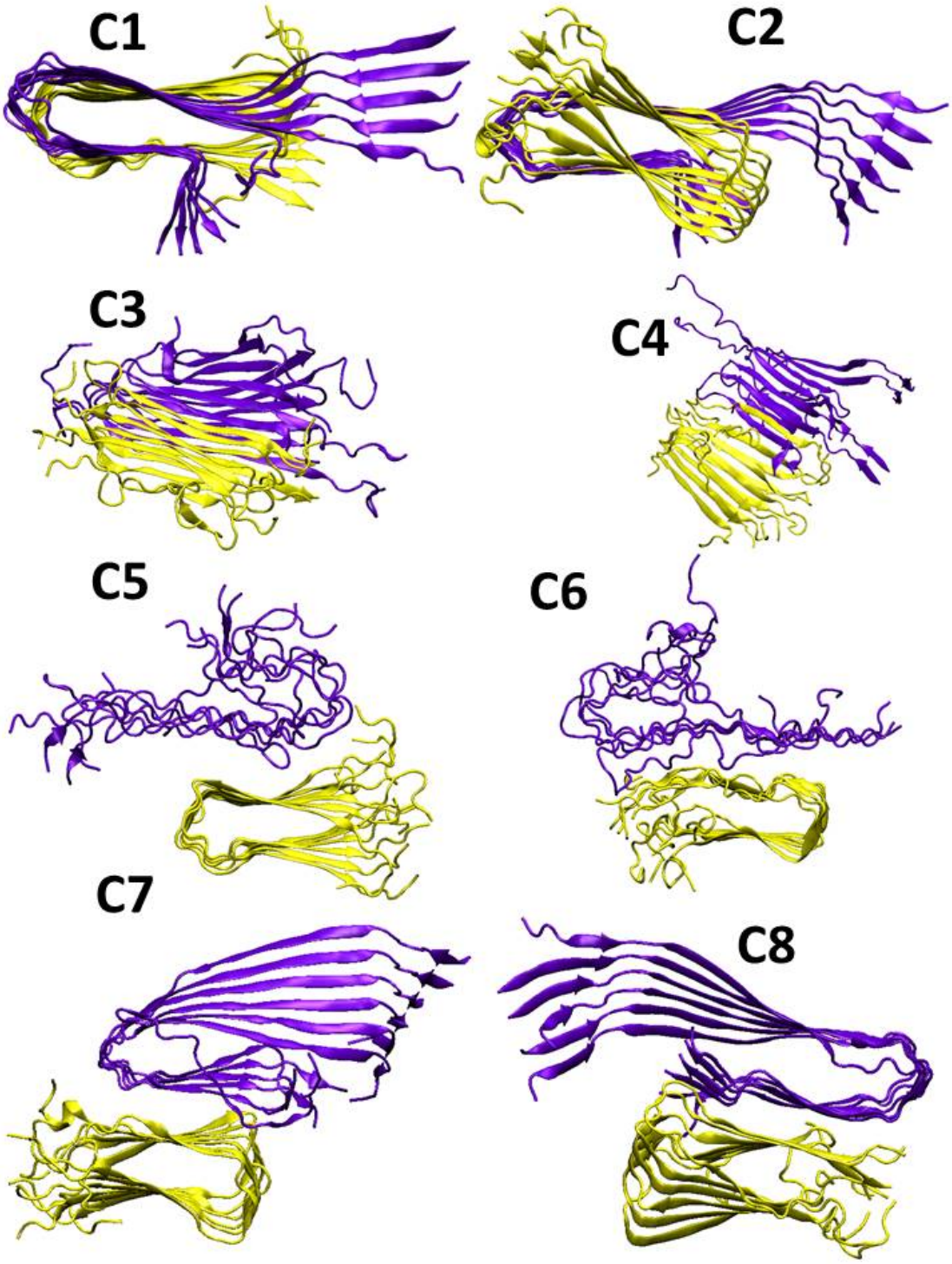

Figure S6: Simulated $A\beta_{1\text{-}42}$-$Amylin_{1\text{-}37}$ dodecamers.

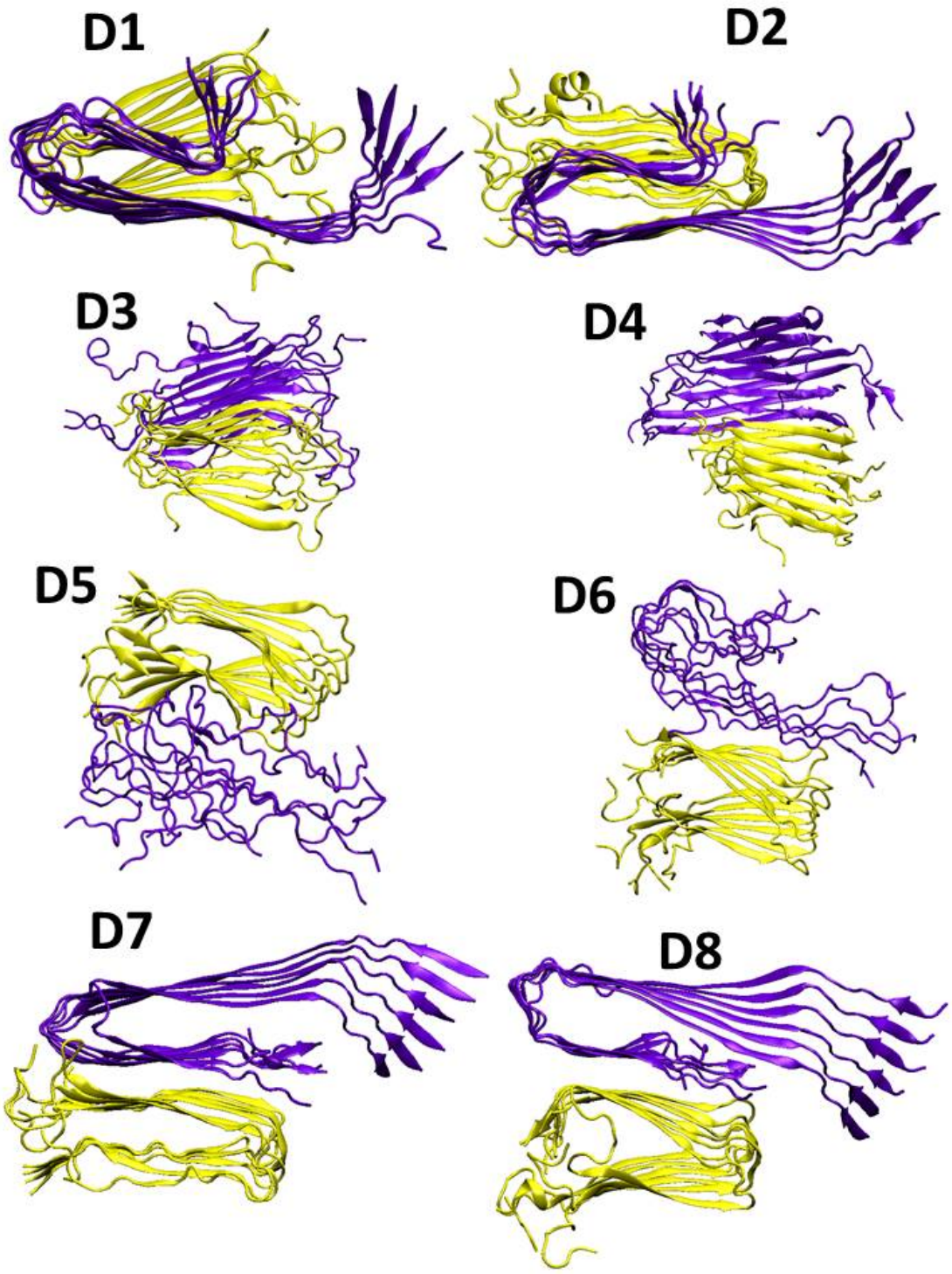

Figure S7: Simulated $A\beta_{1\text{-}42}$-$Amylin_{1\text{-}37}$ dodecamers.

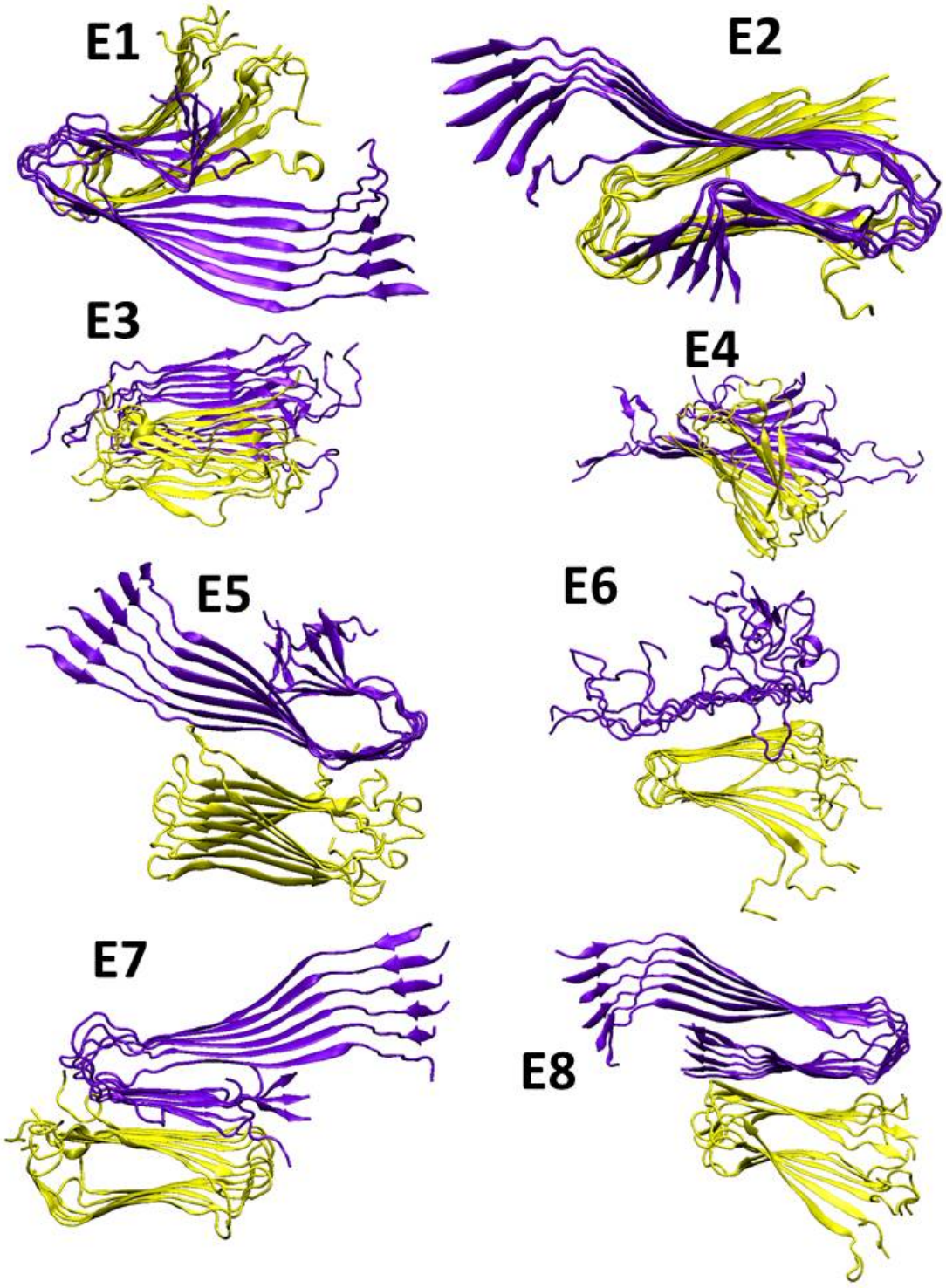

Figure S8: Simulated $A\beta_{1\text{-}42}$-$Amylin_{1\text{-}37}$ dodecamers.

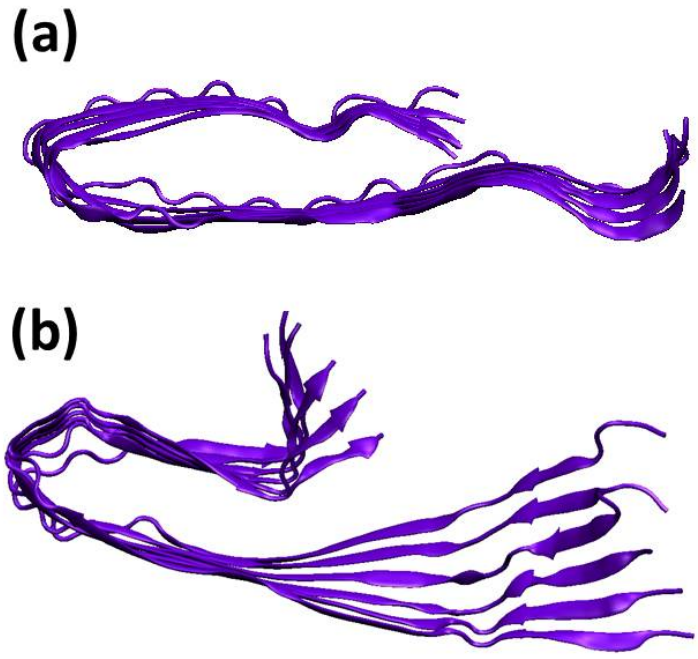

Figure S9: Initial (a) and simulated (b) $A\beta_{1\text{-}42}$ hexamers.

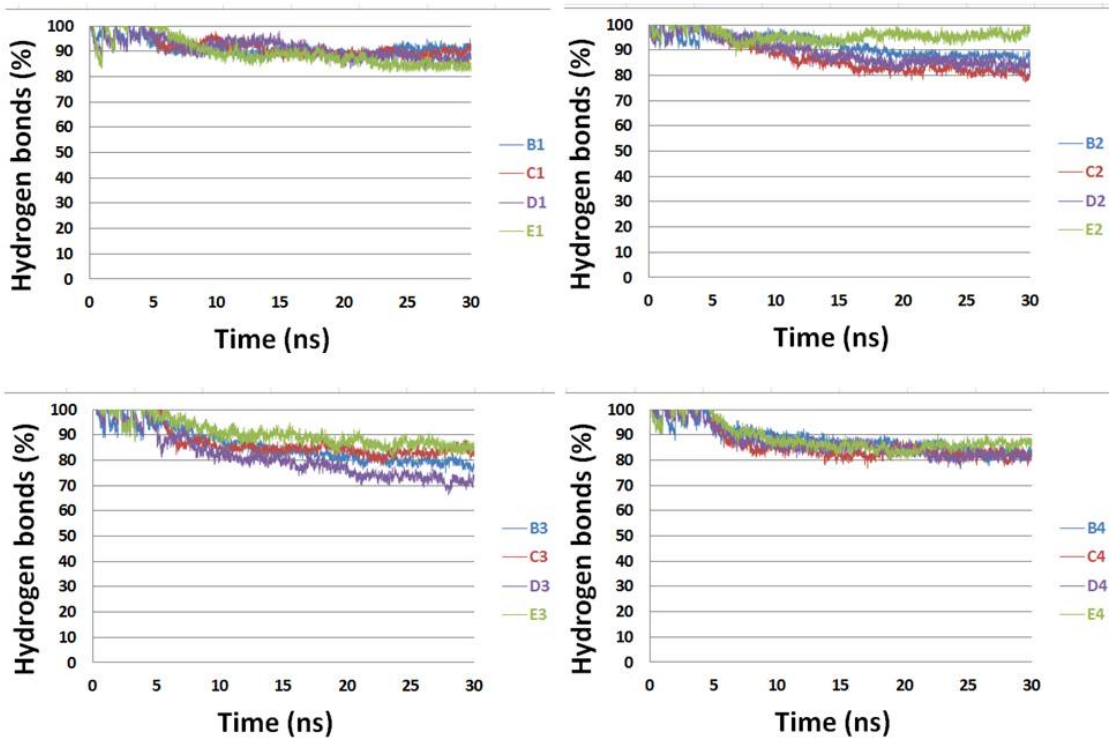

Figure S10: The fraction of the number of hydrogen bonds (in percentage) between all β-strands compare to the number in the initial constructed models $A\beta_{1\text{-}42}$-$Amylin_{1\text{-}37}$ dodecamers.

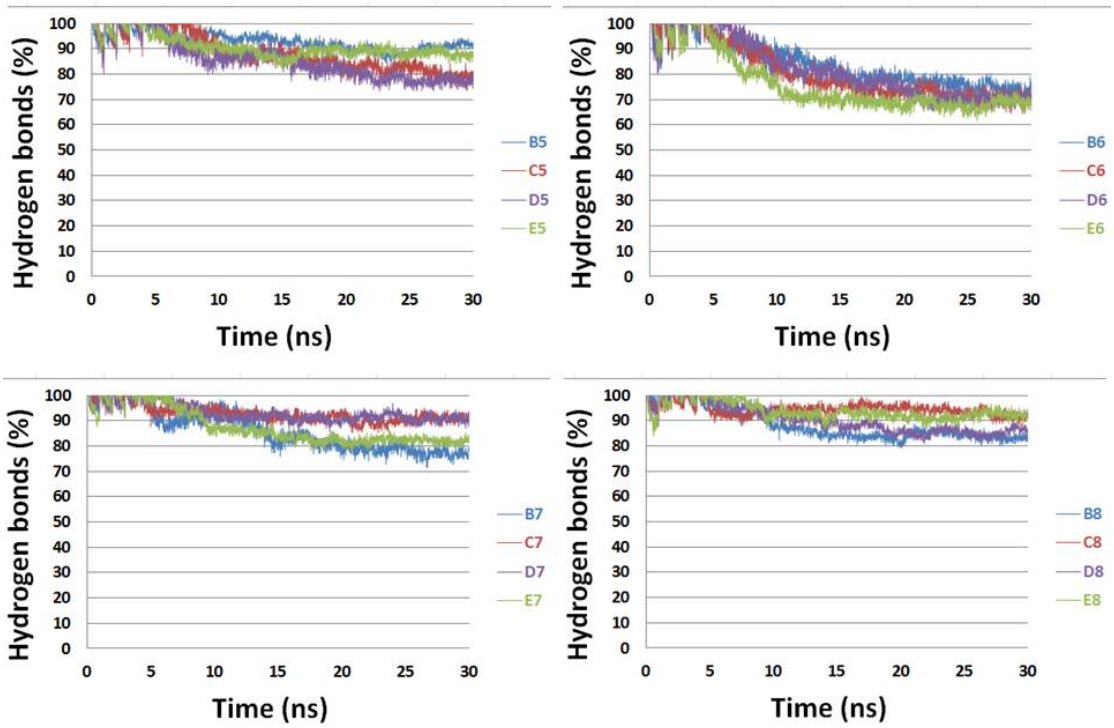

Figure S11: The fraction of the number of hydrogen bonds (in percentage) between all β-strands compare to the number in the initial constructed models of $A\beta_{1-42}$-$Amylin_{1-37}$ dodecamers.

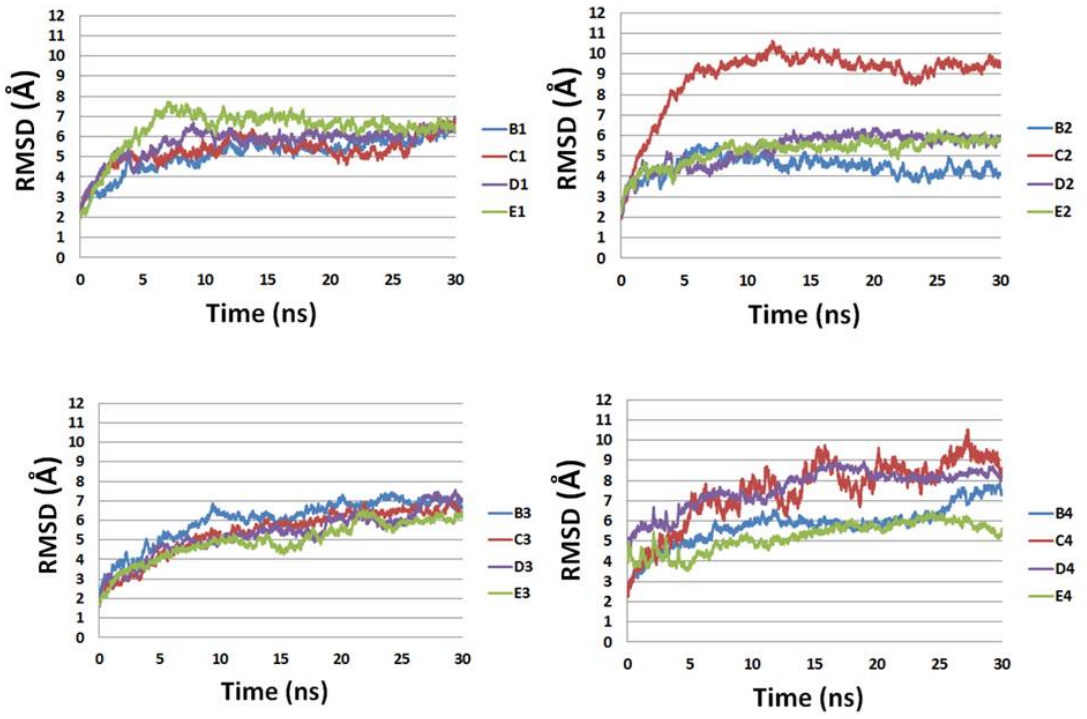

Figure S12: RMSDs of $A\beta_{1\text{-}42}$ hexamers in the $A\beta_{1\text{-}42}$-$Amylin_{1\text{-}37}$ dodecamers.

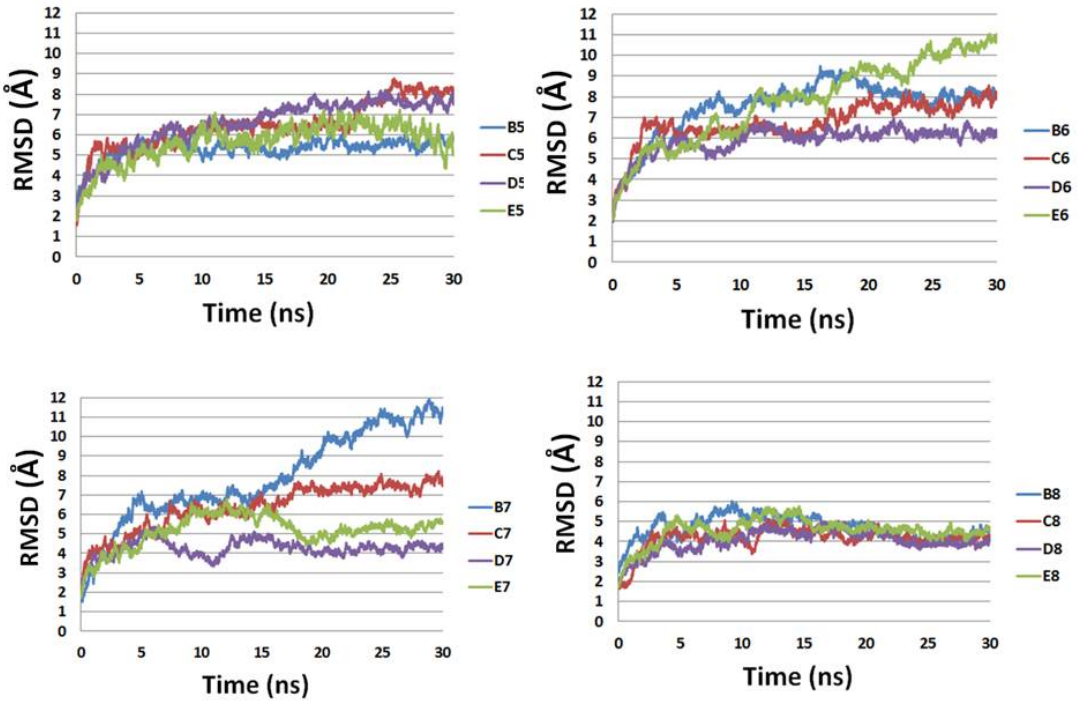

Figure S13: RMSDs of $A\beta_{1\text{-}42}$ hexamers in the $A\beta_{1\text{-}42}$-$Amylin_{1\text{-}37}$ dodecamers.

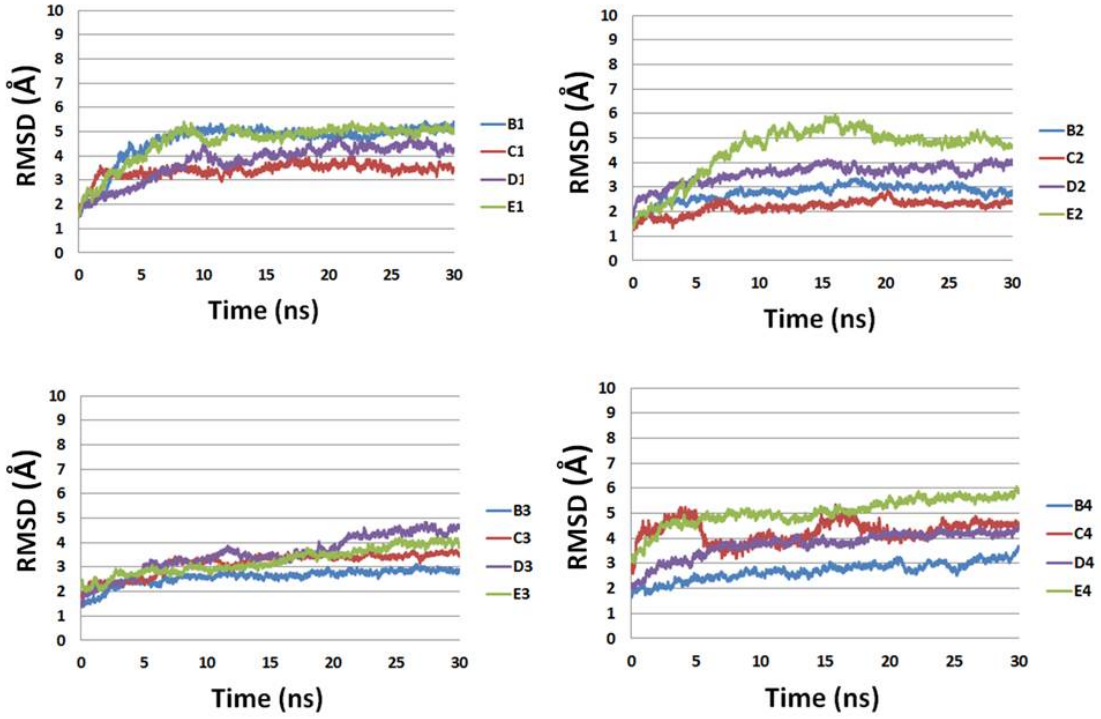

Figure S14: RMSDs of Amylin hexamers in the $A\beta_{1\text{-}42}$-$Amylin_{1\text{-}37}$ dodecamers.

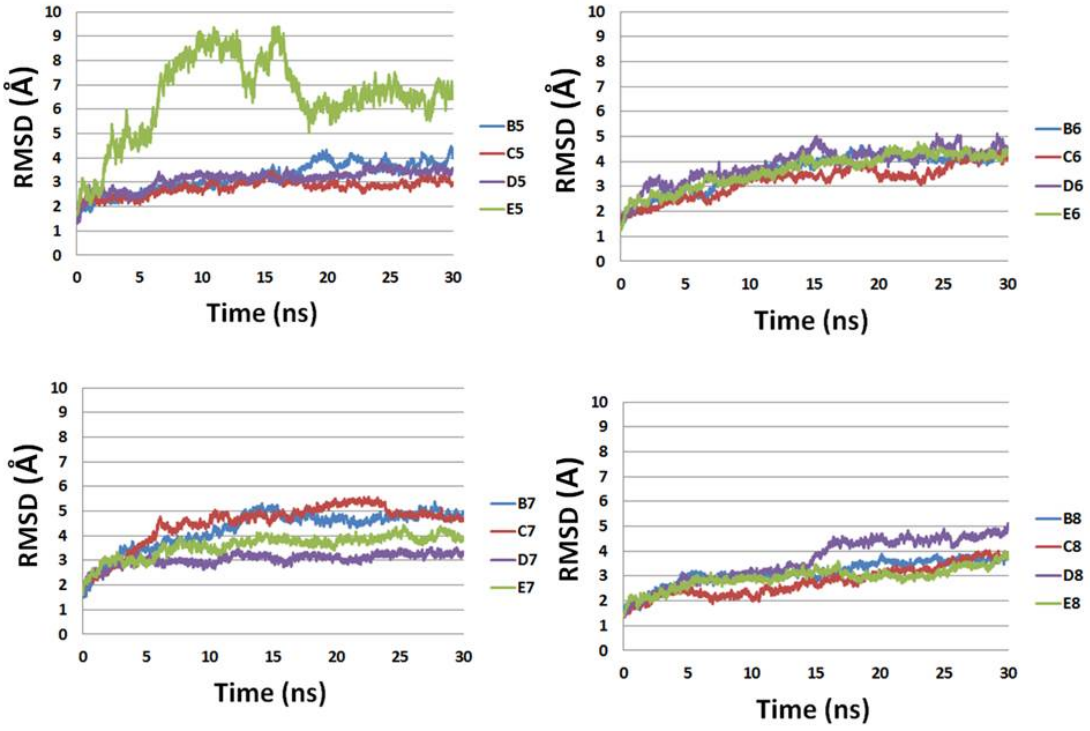

Figure S15: RMSDs of Amylin hexamers in the $A\beta_{1\text{-}42}$-$Amylin_{1\text{-}37}$ dodecamers.

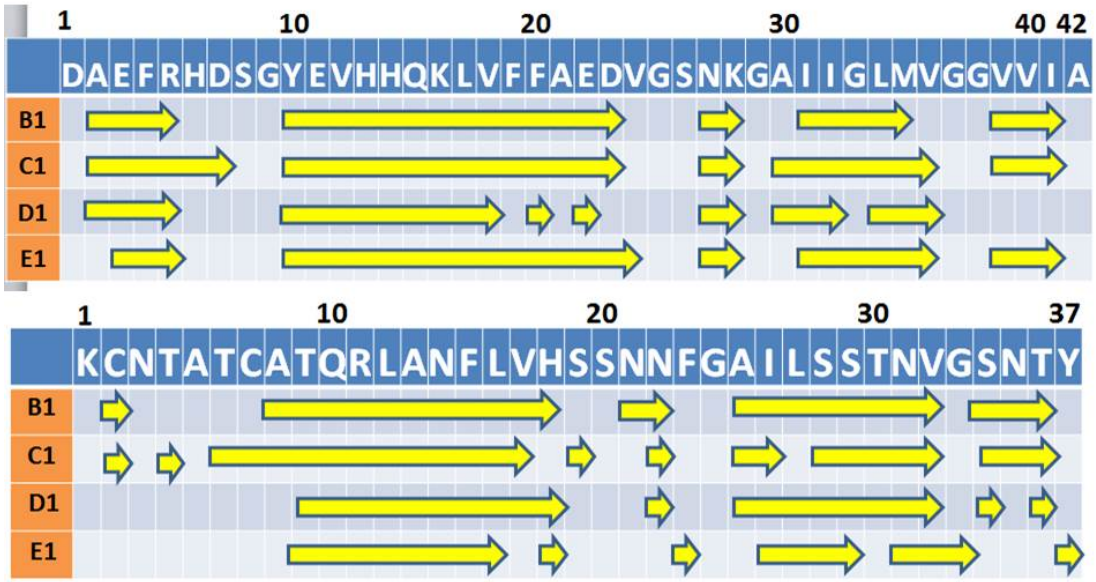

Figure S16: The secondary structure of the simulated models along the sequence of Aβ and Amylin in the cross-seeding $A\beta_{1\text{-}42}$-$Amylin_{1\text{-}37}$ dodecamers. The arrows illustrate β-strand structure.

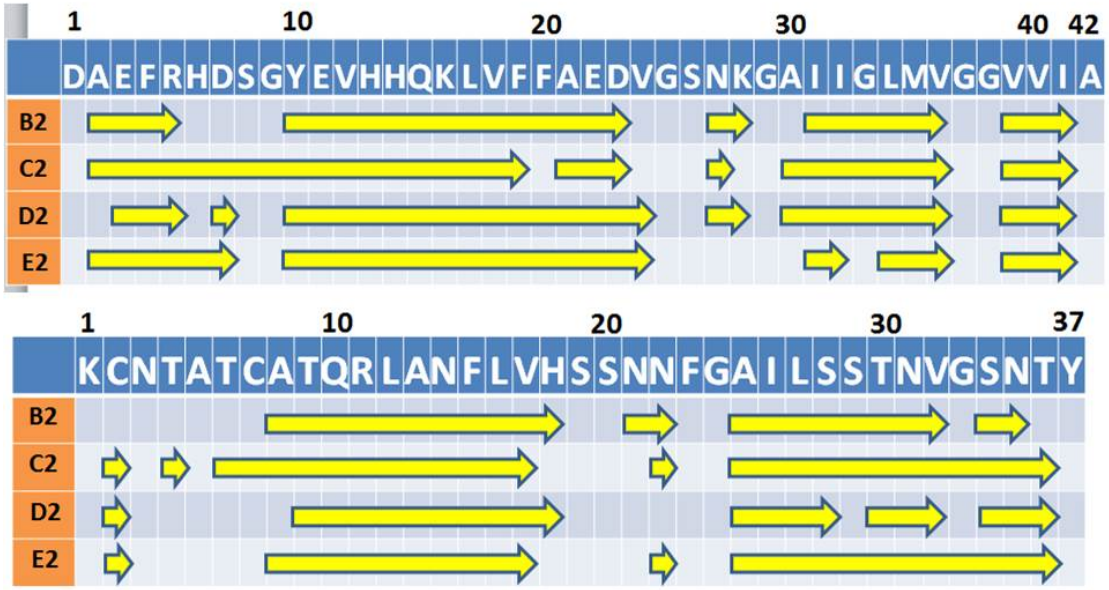

Figure S17: The secondary structure of the simulated models along the sequence of Aβ and Amylin in the cross-seeding $A\beta_{1\text{-}42}$-$Amylin_{1\text{-}37}$ dodecamers. The arrows illustrate β-strand structure.

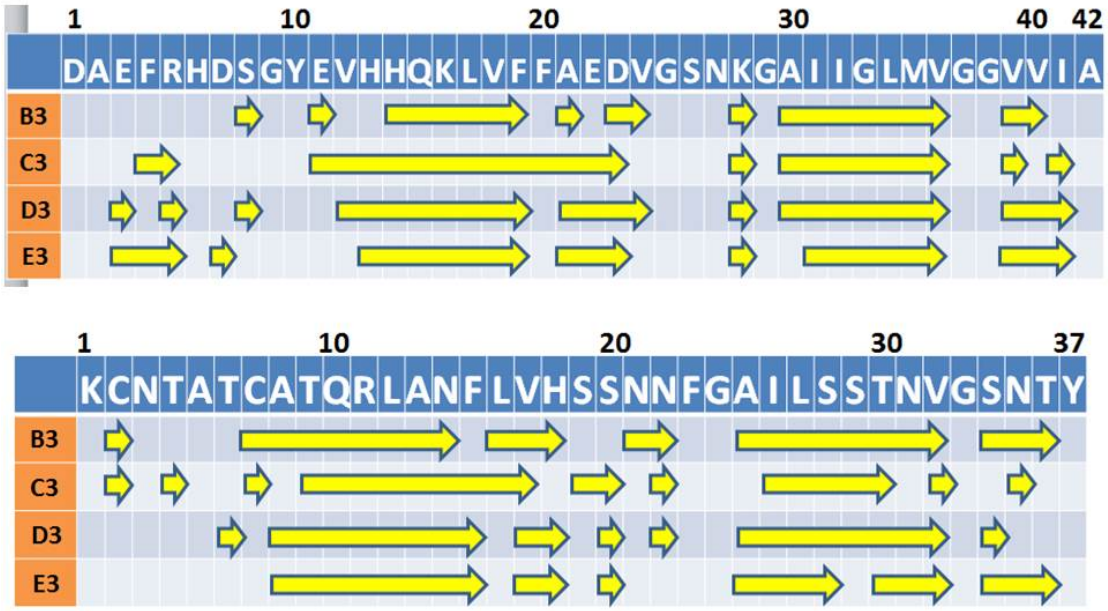

Figure S18: The secondary structure of the simulated models along the sequence of Aβ and Amylin in the cross-seeding $A\beta_{1\text{-}42}$-$Amylin_{1\text{-}37}$ dodecamers. The arrows illustrate β-strand structure.

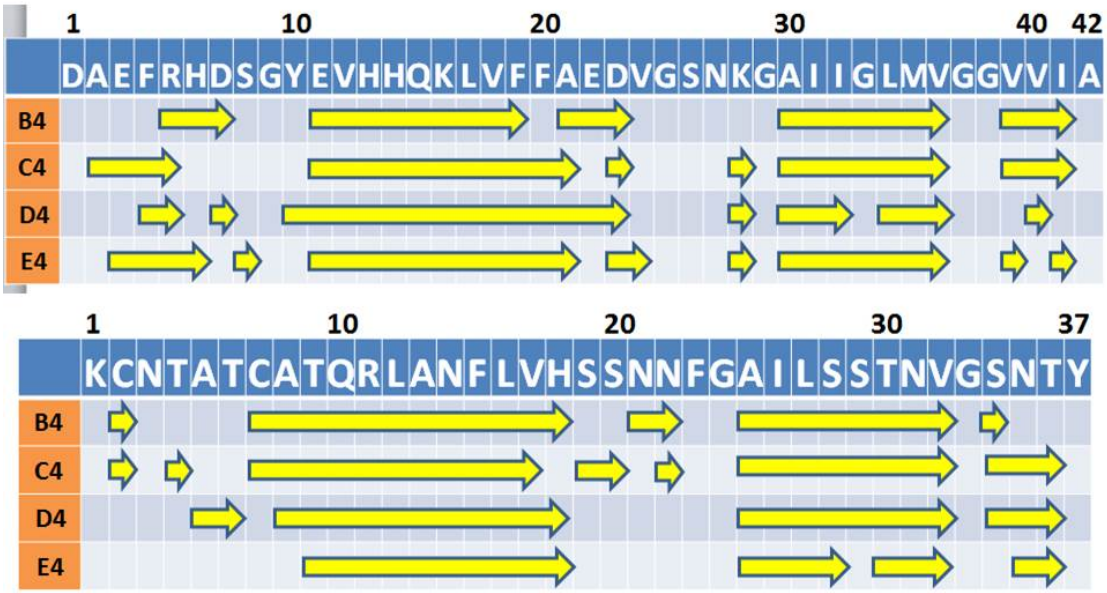

Figure S19: The secondary structure of the simulated models along the sequence of Aβ and Amylin in the cross-seeding $A\beta_{1\text{-}42}$-$Amylin_{1\text{-}37}$ dodecamers. The arrows illustrate β-strand structure.

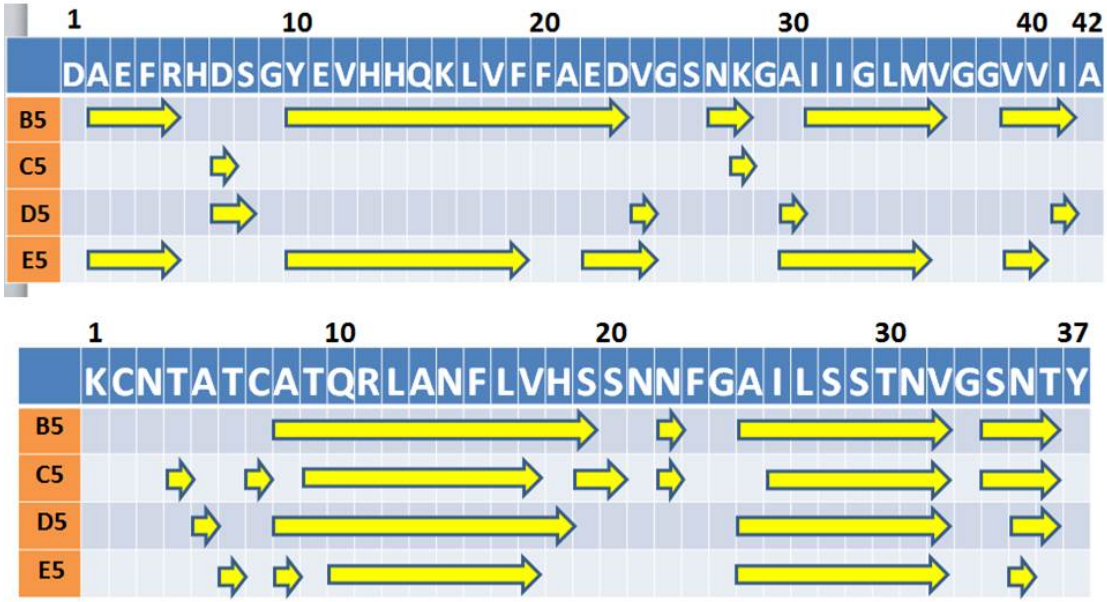

Figure S20: The secondary structure of the simulated models along the sequence of Aβ and Amylin in the cross-seeding $A\beta_{1\text{-}42}$-$Amylin_{1\text{-}37}$ dodecamers. The arrows illustrate β-strand structure.

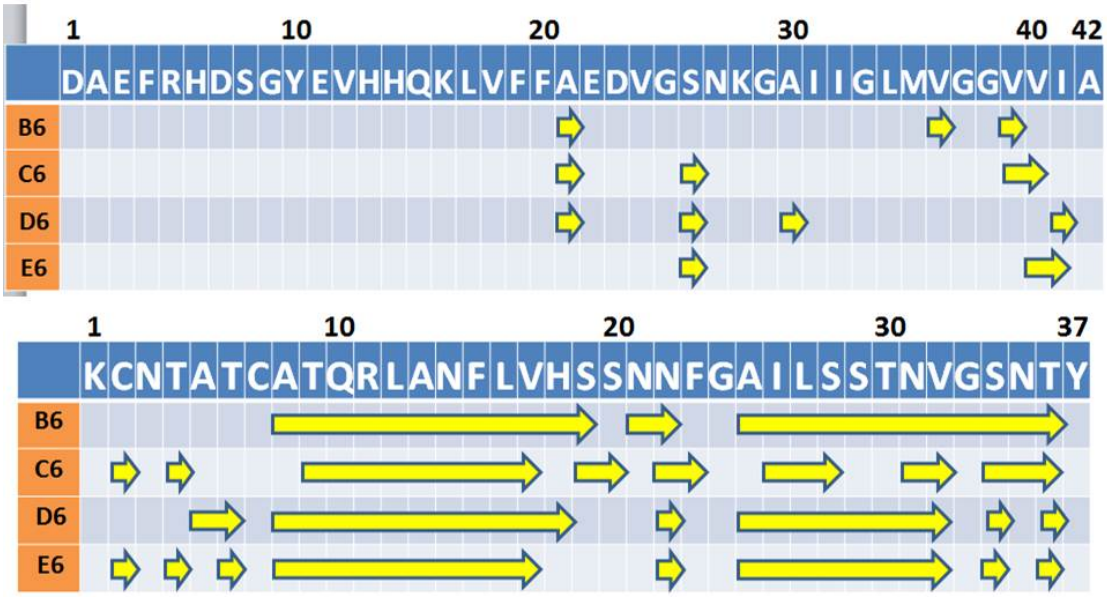

Figure S21: The secondary structure of the simulated models along the sequence of Aβ and Amylin in the cross-seeding $A\beta_{1\text{-}42}$-$Amylin_{1\text{-}37}$ dodecamers. The arrows illustrate β-strand structure.

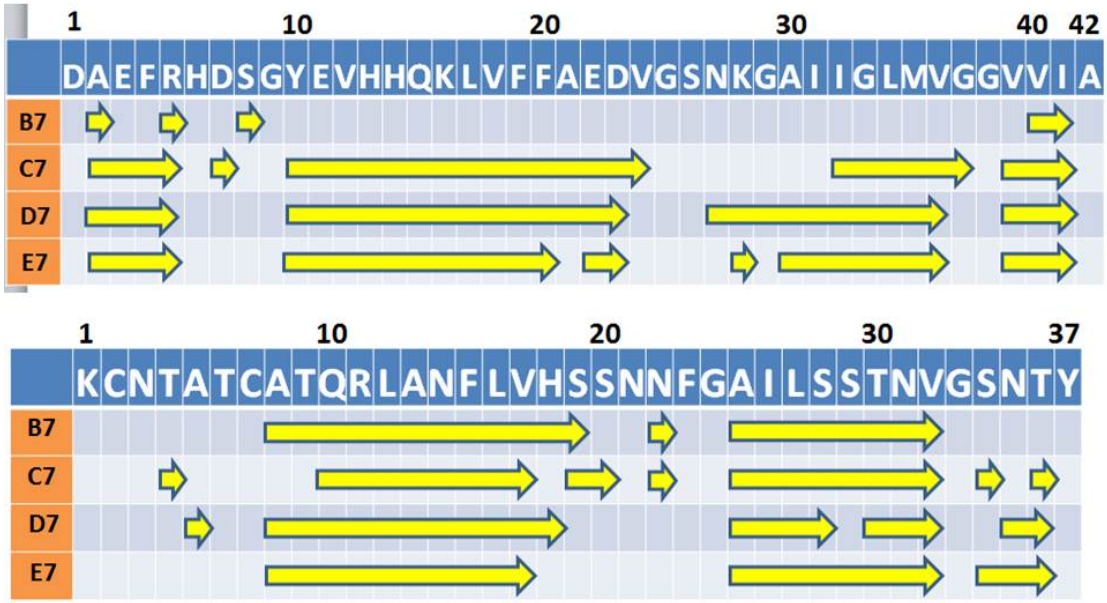

Figure S22: The secondary structure of the simulated models along the sequence of Aβ and Amylin in the cross-seeding $A\beta_{1\text{-}42}$-$Amylin_{1\text{-}37}$ dodecamers. The arrows illustrate β-strand structure.

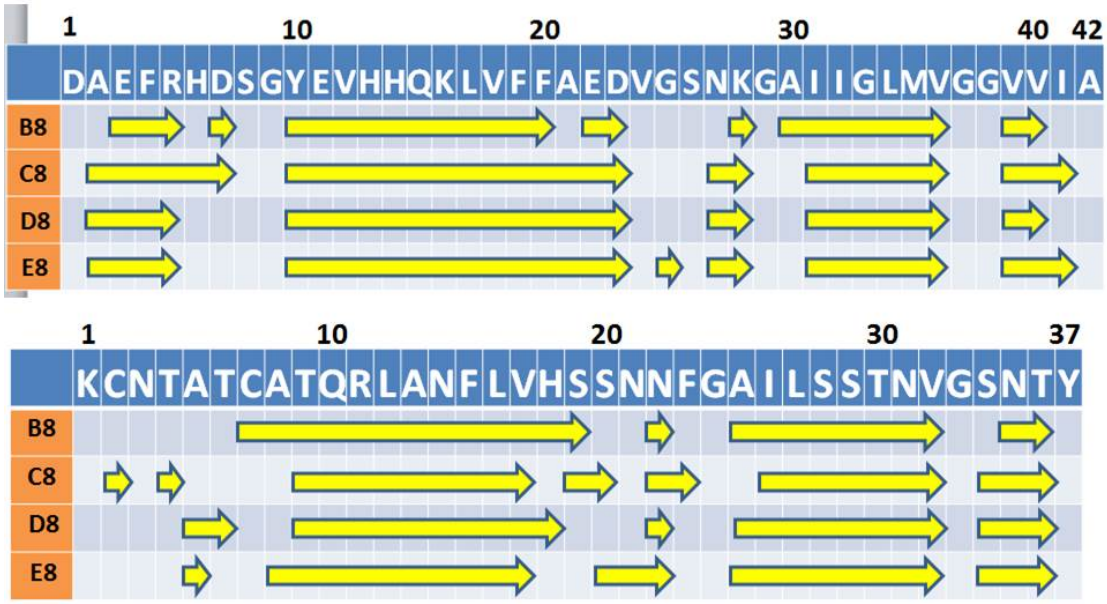

Figure S23: The secondary structure of the simulated models along the sequence of Aβ and Amylin in the cross-seeding $A\beta_{1\text{-}42}$-$Amylin_{1\text{-}37}$ dodecamers. The arrows illustrate β-strand structure.

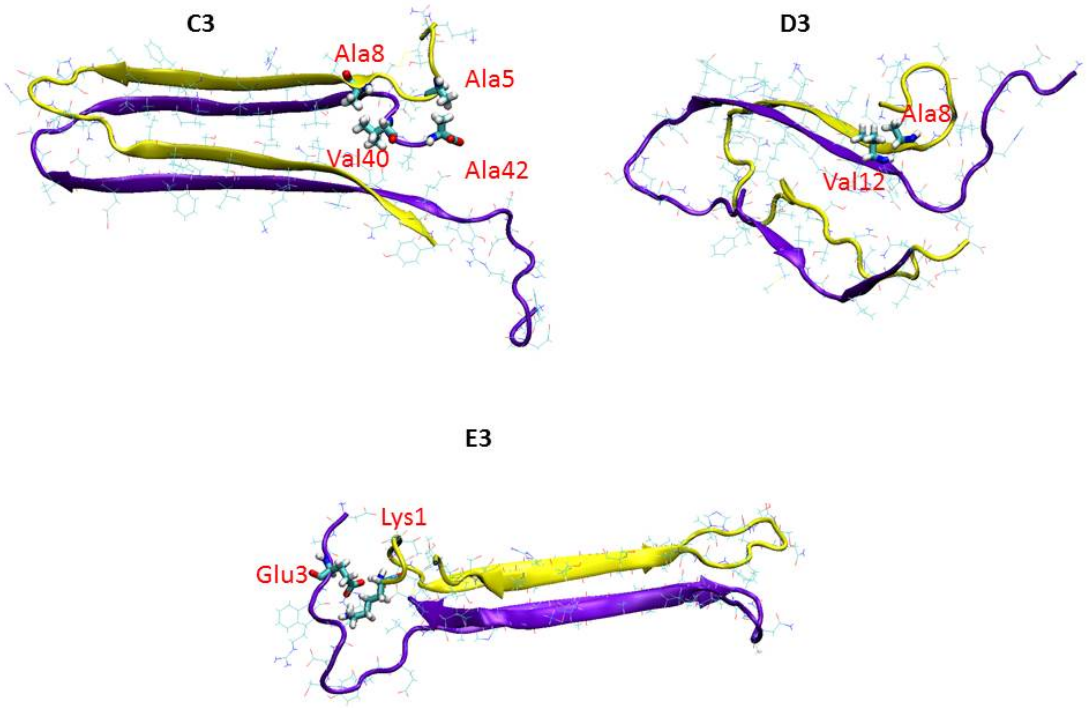

Figure S24: The single layer conformations of models C3, D3 and E3 illustrate intermolecular hydrophobic and electrostatic interactions between $A\beta_{1\text{-}42}$ monomer and $Amylin_{1\text{-}37}$ monomer that stabilize the cross-seeding $A\beta_{1\text{-}42}$-$Amylin_{1\text{-}37}$ oligomers. Only the monomers are seen in the figure.

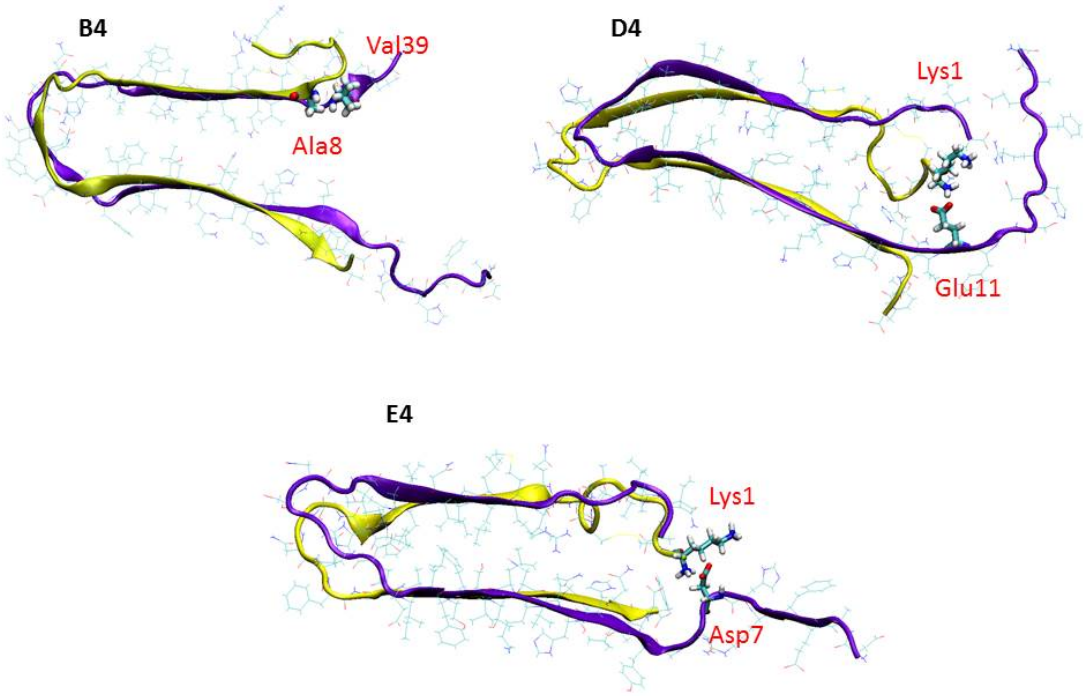

Figure S25: The single layer conformations of models B4, D4 and E4 illustrate intermolecular hydrophobic and electrostatic interactions between $A\beta_{1\text{-}42}$ monomer and $Amylin_{1\text{-}37}$ monomer that stabilize the cross-seeding $A\beta_{1\text{-}42}$-$Amylin_{1\text{-}37}$ oligomers. Only the monomers are seen in the figure.

E5

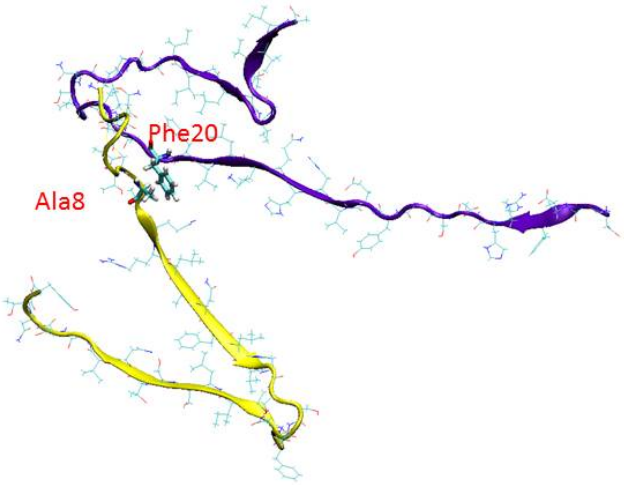

Figure S26: A double conformations of model E5 illustrate intermolecular hydrophobic interactions between $A\beta_{1-42}$ monomer and $Amylin_{1-37}$ monomer that stabilize the cross-seeding $A\beta_{1-42}$-$Amylin_{1-37}$ oligomers. Only the monomers are seen in the figure.

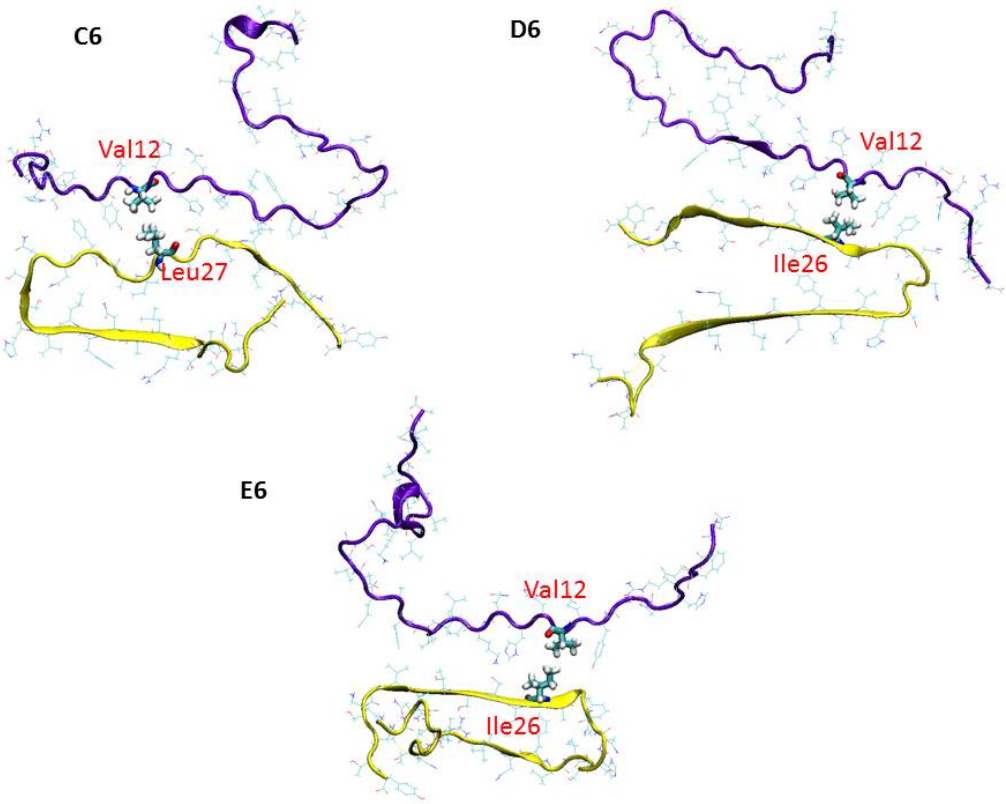

Figure S27: The double layer conformations of models C6, D6 and E6 illustrate intermolecular hydrophobic interactions between $A\beta_{1-42}$ monomer and $Amylin_{1-37}$ monomer that destabilize stabilize $A\beta_{1-42}$ oligomers and do not affect the stabilization of $Amylin_{1-37}$ oligomers. Only the monomers are seen in the figure.

References:

(1) Wineman-Fisher, V.; Atsmon-Raz, Y.; Miller, Y.: Orientations of residues along the beta-arch of self-assembled amylin fibril-like structures lead to polymorphism. *Biomacromolecules* **2015**, *16*, 156-65.
(2) Luca, S.; Yau, W. M.; Leapman, R.; Tycko, R.: Peptide conformation and supramolecular organization in amylin fibrils: constraints from solid-state NMR. *Biochemistry* **2007**, *46*, 13505-22.
(3) Wiltzius, J. J.; Sievers, S. A.; Sawaya, M. R.; Cascio, D.; Popov, D.; Riekel, C.; Eisenberg, D.: Atomic structure of the cross-beta spine of islet amyloid polypeptide (amylin). *Protein science : a publication of the Protein Society* **2008**, *17*, 1467-74.
(4) Petkova, A. T.; Yau, W. M.; Tycko, R.: Experimental constraints on quaternary structure in Alzheimer's beta-amyloid fibrils. *Biochemistry* **2006**, *45*, 498-512.